Journal of Engg. Research **Vol. 4 No. (3) September 2016** pp. 114-127

شبيه موصل معدني مكمل لمرشح يمرر الموجة لأجهزة تردد الراديو ذات التكلفة الفعالة

محمد عارف سبحان بويان، مستورة بنتي عمر، مأمون بن رياض،
نور فضيلة كمال وسوال حامد علي
قسم الهندسة الكهربائية، الهندسة الكهربائية وأنظمة، جامعة كبانغسان ماليزيا،
بانغي، سيلانغور، ماليزيا

الخلاصة

المرشح الممرر للموجة هو جزء لا يتجزأ من كل جهاز إرسال واستقبال لاسلكي. استخدام اللفائف الحلزونية في المرشحات التي تمرر الموجات لا يمكن أن تتغلب على قيود مثل الخسارة الناجمة عن الاثار الطفيلية، المساحة الكبيرة للرقائق، انخفاض عامل الجودة، عدم دقة الضبط، الخ .. لذلك، تعرض هذه الورقة تصميم مغو نشط مبني على أساس المرتبة الثانية لمرشح التمرير في 0.18 ميكروميتر في شبيه موصل معدني تكميلي (CMOS) لتطبيقات ترددات الراديو 2.4 غيغاهرتز. التردد الوسط للمرشح المقترح يمكن تعديله من 1.86 غيغاهيرتز إلى 3.33 غيغاهرتز مع معامل Q مقداره 250 عند تردد مقداره 2.45 غيغاهيرتز. هذا الفلتر يبدد فقط 3.407 ملي واط عند مرور تيار كهربائي 1.5 فولت ويشغل مساحة للرقاقة مقدارها 0.0014 مم^2 فقط.

A complementary metal oxide semiconductor (CMOS) band-pass filter for cost-efficient radio frequency (RF) appliances

Mohammd Arif Sobhan Bhuiyan*, Mastura Binti Omar, Mamun Bin Ibne Reaz, Noorfazila Kamal and Sawal Hamid Md Ali

Department of Electrical, Electronic and Systems Engineering, Universiti Kebangsaan Malaysia, 43600 Bangi, Selangor, Malaysia.

**Corresponding Author: Email: asobhan@eng.ukm.my*

ABSTRACT

A band pass filter is an inherent part of every radio frequency (RF) transceiver. The usage of spiral inductors in band-pass filters cannot overcome limitations such as loss due to parasitic effects, large chip area, low quality factor, less tenability, etc. Therefore, this paper presents an active inductor based design of a second order band-pass filter in 0.18µm complementary metal oxide semiconductor (CMOS) technology for 2.4 GHz radio frequency (RF) applications. The centre frequency of the proposed band pass filter can be adjusted from 1.86 GHz to 3.33 GHz with high Q factor of 250 at 2.45GHz. This filter dissipates only 3.407 mW at 1.5V supply voltage and occupies only 0.0014 mm^2 chip area.

Keywords: Active inductor; band-pass filter; complementary metal oxide semiconductor; integrated circuits; radio frequency.

INTRODUCTION

Increased level of integration is the current trend of modern devices to compensate their price, size and portability (Bhuiyan *et al.,* 2014; Arifin *et al.,* 2012; Jalil *et al.,* 2013; Bhuiyan *et al.,* 2016). The recent development of CMOS technology enables scientists all over the world to manufacture low power, small size and low cost wireless devices for different applications such as RFID, Bluetooth, Zigbee, Wi-Fi, WLAN etc. (Aziz *et al.,* 2013; Uddin *et al.,* 2013; Idris *et al.,* 2013; Bhuiyan *et al.,* 2015).

Analog radio frequency (RF) band-pass filter is an important module in RF transceivers. The performance of band-pass filter severely influences the performance of the whole transceiver as it directly connects antenna to the transceiver. Band-pass filter is a type of device or electronic circuitry that allows only specific signals or frequencies to pass through it but stops the unwanted signals or frequencies. Band-pass filters are usually implemented with passive inductors (Aljarajreh *et al.,* 2013). But regrettably, the parasitic effects, for instance coupling capacitance and losses

associated to the substrate demean the performance of the filter. These difficulties have been addressed by utilizing different techniques, such as geometry improvements and patterned ground shields, whereas the Q-factor of on-chip spiral inductors is still inadequate (usually less than 20) (Yu *et al.,* 2003) in standard CMOS technology. Moreover, passive inductors are difficult to fabricate in IC which may result in large chip area, low-quality factor, less tunability etc. (Wang *et al.,* 2012). These effects become crucial, especially in the case of silicon substrate. Although integrated circuit technology is experiencing rapid improvements in recent years, the use of passive inductors is decreasing day by day (Krishnamurthy *et al.,* 2010; Ren & Benedik, 2013).

In order to overcome the margins, active inductor based bandpass filters have been introduced. Active inductors can constantly tune to protect temperature or process variations. Beyond that, active inductor only takes about 1% - 10% of passive active inductor area, which can produce smaller chip area and cost. Besides, they also have higher inductance value, wide frequency tuning range and higher quality factor, which are essential for different circuit designs (Andriesei *et al.,* 2009). Moreover, compared to Gm-C and Q enhanced LC tank band-pass filters, filters with active inductor show better performance in terms of low power consumption, small silicon area, high Q factor and tunability. In general, it experiences higher noise and very bad linearity (Bakken & Choma, 2003). Band-pass filters are used in varieties of applications including mobile phones (GSM 900/1800), global position system, wireless local area network, bluetooth, zigbee, television broadcasting, radio frequency identification (RFID) and many more (Kuhn *et al.,* 2003).

In this paper, all-transistors differential band-pass filter in 0.18µm CMOS technology is proposed. Avoidance of passive components, proper transistor optimization in differential active inductor structures are used to obtain better performance. This also leads to achieve very small chip size. The proposed filter will be very useful for RF transceivers for diverse applications.

METHODOLOGY

Realization of active inductor

To design active inductor circuit operating above 1GHz, generally op-amps and transconductors (g_ms) with linearization methods cannot be adopted, as these techniques generally create extra internal poles, phase shifts and parasitic capacitance (Xiao & Schaumann, 2007). Instead, active or passive inductor circuits can be used. Because of limitations of passive inductances, active inductors are more suitable for low power compact devices. The realization of an active inductor relies on the basic gyrator theory, where two transconductors are connected end-to-end and one end of the gyrator is bonded to a capacitor as shown in Figure 1 (Wu *et al.,* 2003).

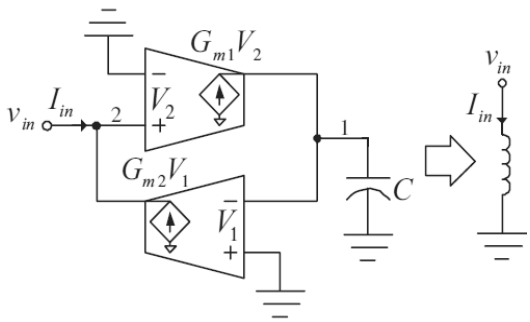

Fig. 1. Basic concept of a gyrator.

where, G_{m1} and G_{m2} are the transconductances. The admittance into port 2 of Gm-C arrangement is given by

$$Y = \frac{I_{in}}{V_2} = \frac{1}{s\left(\frac{C}{g_{m1}g_{m2}}\right)} \tag{1}$$

Port 2 of the Gm-C arrangement become as single ended inductor where the inductance is given by

$$L_{eq} = \frac{C}{g_{m1}g_{m2}} \tag{2}$$

The inductance is, therefore, inversely proportional to the product of the transconductors and directly proportional to the value of the capacitor.

Karsilayan Schauman active inductors

To implement the band-pass filter, Karsilayan Schauman active inductor (KSAI) circuit architecture is proposed. The KSAI consist of common source transconductance as a negative transconductnce and differential pair transconductance as a positive feedback transconducatance as shown in Figure 2 (Córdova *et al.,* 2009).

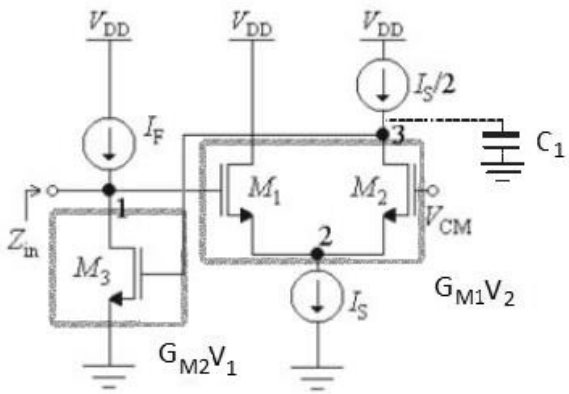

Fig. 2. KSAI circuit architecture.

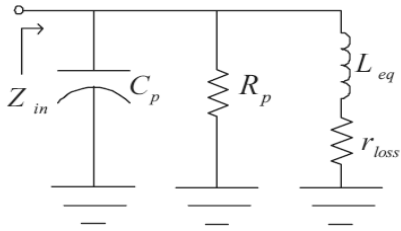

Fig. 3. Equivalent RLC circuit

In Figure 2, transistor M3 has a negative transconductance labelled –Gm2 (-gm3) with input voltage at node 3 and output current at node 1. Transistor M1 and M2 forms a positive transconductance labelled Gm1 (0.5gm1 if gm2=gm1) with input voltage at node 1 and output current at node 3. Hence, -Gm2 and Gm1 forms the gyrator, which in turn form an inductor at node 1 along with the parasitic capacitor C1 at node 3. This KSAI circuit can be represented as an RLC circuit as shown in Figure 3.

The small signal circuit of KSAI is shown in Figure 4. Here, it is considered that gm1−3 being transconductances of M1−3, C1−3 and g1−3 are the total parasitic capacitances/conductances at nodes 1-3, respectively.

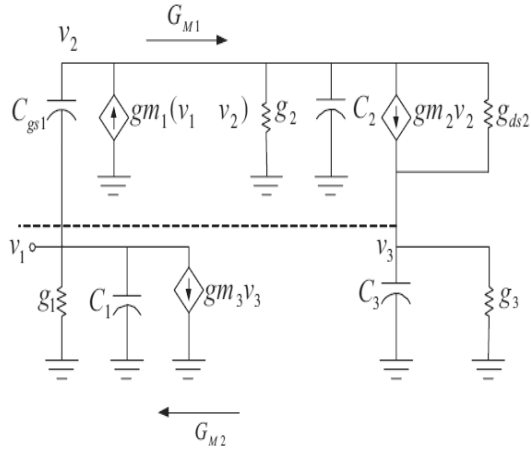

Fig. 4. AC small signal equivalent circuit

From Figure 4, the approximate magnitude of input impedance (Zin) is

$$Z_{in}(s) = \frac{\frac{s}{C_1} + \frac{g_3}{C_1 C_3}}{s_2 + s\left(\frac{g_1}{C_1} + \frac{g_1 g_3 C_2}{C_1 C_3 G} - \omega_2 \frac{C_2}{G}\right) + \frac{g_{m2} g_{m1} g_{m3}}{G C_1 C_3}} \quad (3)$$

Where, g_{m1} and g_{m2} are the transconductances of the two amplifiers and G = gm1 + gm2 + g2. The input impedance confirms that it is equivalent to an RLC network, as shown in Figure 3. The element values can be determined as follows. To simplify

the following expressions the value of g2 is considered nearly zero, because the conductance at node 2 corresponds to the current source I1 in Figure 2. For a dc level (s=0),

$$Z_{in}(0) = \frac{g_3 G}{g_{m2} g_{m1} g_{m3}} \approx \frac{g_3}{0.5 g_{m1} g_{m3}} = r_{loss} \tag{4}$$

When gm1 ≈ gm2 and g2 << gm1, gm2, the parallel resistor, capacitor and transconductance are

$$C_p = C_1 \tag{5}$$

$$R_p = \frac{1}{g_1} \tag{6}$$

$$G = g_{m1} g_{m2} \tag{7}$$

The equivalent inductance is

$$L_{eq} = \frac{GC_3}{g_{m1} g_{m2} g_{m3}} \approx \frac{C_3}{0.5 g_{m1} g_{m3}} \tag{8}$$

The resonance frequency ω is

$$\omega = \sqrt{\frac{0.5 g_{m1} g_{m3}}{C_1 C_3}} = \frac{1}{\sqrt{L_{eq} C_1}} \tag{9}$$

The quality factor, Q at resonance frequency is

$$Q = \sqrt{\frac{\frac{g_{m1} g_{m2} g_{m3}}{GC_1 C_3}}{\frac{g_1}{C_1} + \frac{g_3}{C_5} - \frac{C_2}{G}\left(\omega_2 - \frac{g_1 g_3}{C_1 C_3}\right)}} \tag{10}$$

Band-pass filter realization

The proposed band-pass filter is composed of three stages as shown in Figure 5. The input buffer translates the input signal to a current, which is made to pass through a resonator made of active inductor circuit and the produced voltage is the output. An output buffer (source-follower) is needed to drive the resistive load as well as to prevent the load from severely influencing the filter's f_o and Q.

Fig. 5. Block diagram of the proposed inductor-less Band pass filter.

The complete schematic circuit of the proposed second order differential band pass filter including input and output buffer circuits is shown in Figure 6. The buffer circuits are used to supply sufficient current to and/or from the adjacent circuits and also perform the task of input and output impedance matching at the desired operating frequency band.

The value of Vif, Vis, and Vis2 is varied between 0.8V to 0.9V so that the centre frequency of the filter can be tuned. Value of Vcm is 0.7V whereas the values of Vbias and Vq are 0.6V.

The aspect ratio of the width and length each of the transistor in the second order band pass filter is shown in Table 1.

Table 1. Aspect ratio of CMOS transistors

Transistors	**Aspect ratio (W/L)**
M11,M8	15µ/0.18µ
M15,M12	5µ/0.18µ
M21.M18	5µ/0.18µ
M9,M6	15µ/0.18µ
M13,M10	10µ/0.18µ
M7,M4	20µ/0.18 µ
M2,M1	20µ/0.18µ
M5,M3	20µ/0.18µ
M17,M14	10µ/0.18µ
M43,M20	15µ/0.18µ
M19,M16	15µ/0.18µ

RESULTS AND DISCUSSIONS

The proposed band-pass filter for 2.4 GHz band RF applications is designed and simulated in 0.18-µm CMOS process. Design architect (DA-IC) and IC station tools of Mentor graphics are used to measure its performance. In this study, tunability, centre frequency, Q factor, gain and noise figure of the designed band-pass filter are evaluated and the performances are compared with other researches.

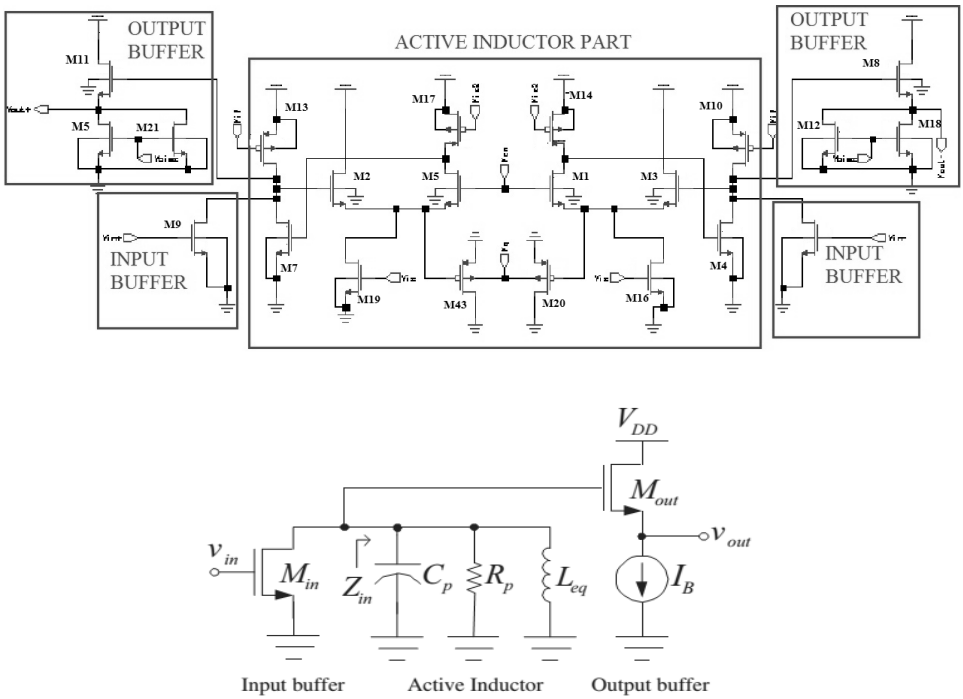

Fig. 6. Complete circuit of the proposed inductor-less band-pass filter along with its single ended passive version.

The centre frequency of the band-pass filter can be tuned by changing the bias voltages and the results are shown in Figure 7. From Figure 7 it is clear that the centre frequency of the band-pass filter can be tuned from 1.85 GHz to 3.33 GHz by varying the voltages Vif, Vis and Vis2 from 0.8V to 0.9V.

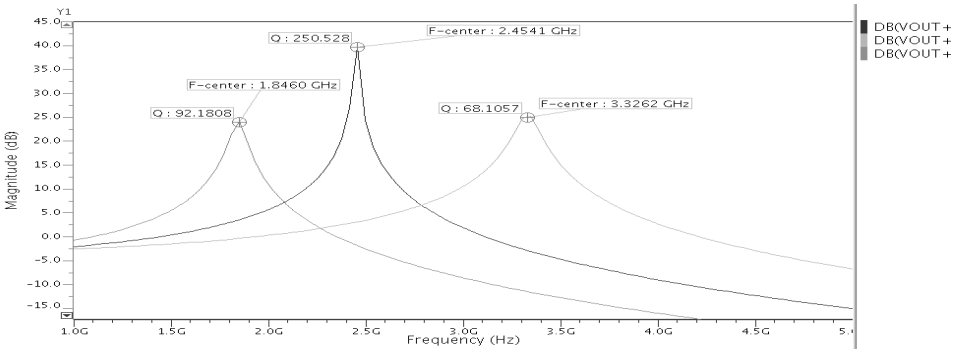

Fig. 7. Tunabilty of centre frequency of the filter

The Q factor of the band-pass filter for different centre frequencies is also shown in Figure 7. From the result, it can be taken into account that the band-pass filter with centre frequency of 2.45GHz has the highest Q factor of 250.5. At 1.84 GHz and 3.32

GHz centre frequency the values of Q factors are 92.18 and 68.10 respectively. Figure 8 shows the sample output and input voltages for the band-pass filter from which the gain of the filter will be computed. The output voltage is 393.76mV (rms value 278.43mV) for the input voltage 500mV (rms value 356.07mV).

Therefore, the voltage gain for band-pass filter in dB is

$$Gain = 10\log\frac{V_{out}}{V_{in}} = -1.068\text{dB} \tag{11}$$

The value of voltage gain of the filter is -1.068, which implies that the filter dissipates power. The total power dissipation together with the biasing, the input buffer and the output buffer is 3.407mW. If the filter is incorporated directly without adjoining the input buffer and the output buffer, it will consume less power.

Figure 9 and Figure 10 illustrate the input and output referred voltage noise for the band-pass filter. The value of input referred voltage noise is 139.59nV/√Hz. The RMS voltage for the input noise voltage is 98.7nV. Whereas, the value of output referred voltage noise is 936.18nV/√Hz and the RMS voltage for the output noise voltage is 661.98nV.

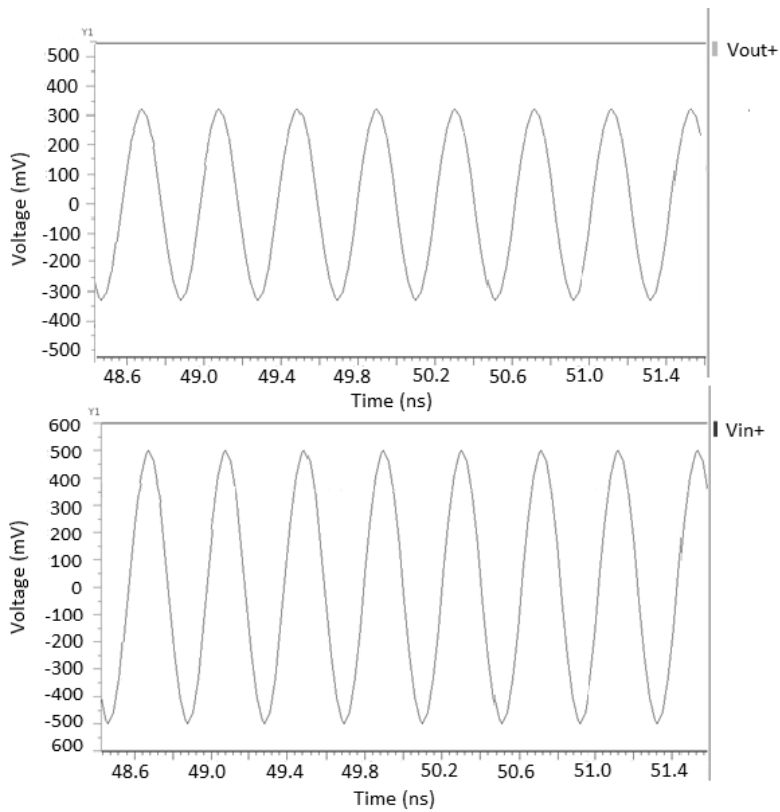

Fig. 8. Output and input voltages of the band-pass filter

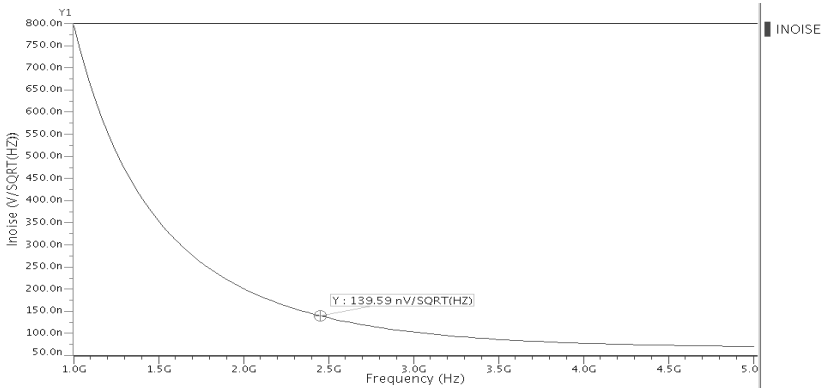

Fig. 9. Input referred voltage noise.

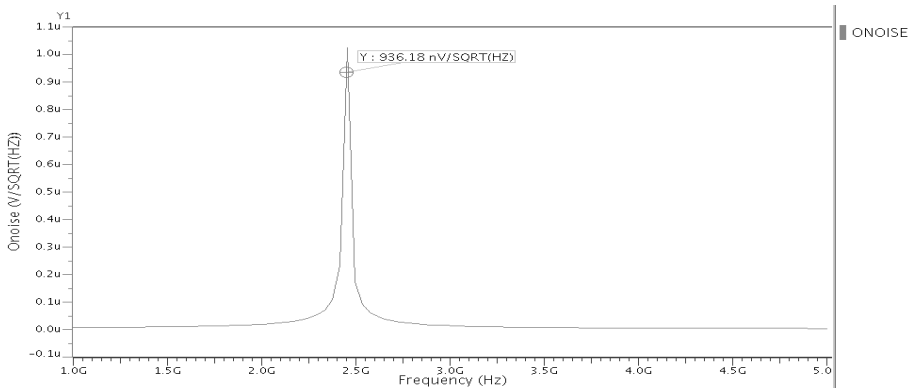

Fig. 10. Output referred voltage noise.

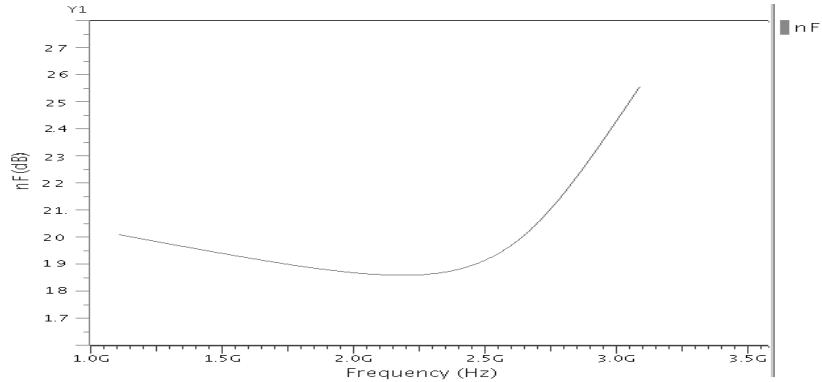

Fig. 11. Noise figure variation of the filter

The noise figure (NF) of the filter as a function of frequency is shown in Figure 11. From the graph it is evident that the NF of the filter is minimal at 2.4 GHz. The noise figure of the band-pass filter at 2.4 GHz can be calculated as

$$SNR_{input} = \frac{V_{\text{rmsinput}}}{V_{\text{rmsinput noise}}} = 3.6076\text{M} \tag{12}$$

$$SNR_{output} = \frac{V_{\text{rmsoutput}}}{V_{\text{rmsoutput noise}}} = 0.421\text{M} \tag{13}$$

$$NF = 20\log\frac{SNR_{input}}{SNR_{output}} = 18.6\,\text{dB} \tag{14}$$

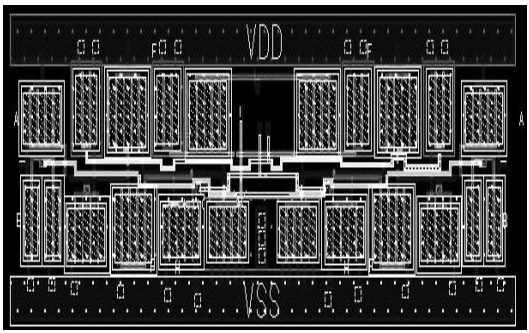

Fig. 12. Layout of second order band pass filter.

Figure 12 shows the layout of the proposed second order band-pass filter. The layout consist of 6 PMOSs and 16 NMOSs. Total number of transistor is 22. The total area of the filter is 0.07mm x 0.02mm i.e., 0.0014 mm^2.

Table 2 shows the comparison of this work to the previous researches of same CMOS process technology to have a fair judgment. From the assessment, it is evident that the proposed filter show very small power dissipation at small power supply voltages and occupies the smallest silicon area compared to the rest of the band-pass filters due to the adaptation of small size of transistors as well as avoidance of passive components like capacitors, resistors etc. Although the proposed band-pass filter suffers from high noise figure compared to the previous works, it manages to have high Q factor of 250 and wide tuning range from 1.85 GHz to 3.3 GHz. The overall performance of the filter indicates that it is very much suitable for low power compact RF devices.

Table 2. Summary of overall performance of active inductors band pass filters.

Parameters	(Choi & Luong, 2001)	(Allidina & Mirabbasi, 2006)	(Weng & Kuo, 2007)	(Gao *et al.,* 2008)	(Chen *et al.,* 2011)	(Lin *et al.,* 2011)	(Xu *et al.,* 2014)	This work
Technology	0.18µm	0.18µm	0.18µm	0.18µm	0.18µm	0.18µm		0.18µm
Filter order	2	2	2	2	-	3	5	2
Centre frequency (GHz)	0.07	0.88 – 3.72	2 – 2.9	1.92-3.82	2.35-3.66	1.58	2.4	1.85-3.33
Power dissipation (mW)	120	26	4	10.8	4.3	14.4	399.3	3.407
Noise figure (dB)	NA	NA	4.3	18	-	15	21.24	18.6
Maximum Q factor	350	300	80	-	-	-		250
Power supply (V)	2.5	1.8	1.5	1.8	1.8	1.8	3.3	1.5
Area (mm^2)	0.96*	0.00805	NA	0.03	0.40*	0.92*	0.15*	0.0014

* Including pads

CONCLUSION

The design of transistor-only band-pass filter in 0.18 µm CMOS technology has been presented. The poor noise performance due to active inductor circuit is offset by less chip area and by excellent electronic tuning. Higher operating frequencies are accomplished by making use of an all-NMOS signal path. This filter can be operated at centre frequency between 1.86GHz until 3.33GHz. This filter also has high Q factor of 250 at 2.45GHz. It consumes only 3.407mW at 1.5V supply and occupies only 0.07mm x 0.02mm chip space. This filter will be a good module for RF devices, which require compactness and wide tuning range.

REFERENCES

Aljarajreh, H., Reaz, M., Amin, M.S. & Husain, H. 2013. An active inductor based low noise amplifier for RF receiver. Electronics and Electrical Engineering, **19**:49-52.

Allidina, K. & Mirabbasi, S. 2006. A widely tunable active RF filter topology. 2006 IEEE International Symposium on Circuits and Systems (ISCAS 2006), Island of Kos, pp.1- 4.

Andriesei, C., Goras, L., Temcamani, F. & Delacressoniere, B. 2009. Wide tuning range active RF band-pass filter with MOS varactors Romanian Journal of Information Science and Technology, **12**:485-495.

Arifin, M., Mamun, M., Bhuiyan, M.A.S. & Husain, H. 2012. Design of a low power and wide band true single-phase clock frequency divider. Australian Journal of Basic and Applied Sciences, **6**: 73-79.

Aziz, F.I.B.A., Mamun, M., Bhuiyan, M.A.S. & Bakar, A.A.A. 2013. A low drop-out voltage regulator in 0.18 µm CMOS technology. Modern Applied Science, **7**:70-76.

Bakken, T. & Choma, J. 2003. Gyrator-based synthesis of active on-chip inductances. Analog Integrated Circuits and Signal Processing, **34**:171-181.

Bhuiyan, M.A.S., Chew, J.X., Reaz, M. & Kamal, N. 2015. Design of an active inductor based LNA in Silterra 130 nm CMOS process technology. Journal of Microelectronics, Electronic Components and Materials, **45**:188-194.

Bhuiyan, M.A.S., Reaz, M., Jalil, J., Rahman, L.F. & Chang, T.G. 2014. Design trends in fully integrated 2.4 GHz CMOS SPDT switches, Current Nanoscience, **10**:334-343.

Bhuiyan, M.A.S., Zijie, Y., Yu, J.S., Reaz, M.B.I., Kamal, N. & Chang, T.G. 2016. Active inductor based fully integrated CMOS transmit/receive switch for 2.4 GHz RF transceiver, Anais da Academia Brasileira de Ciências, **88**:1089-1098.

Chen, S.W., Wu, J.W., Wu, J.D. & Li, J.S. 2011. Tunable active band-pass filter design. Electronics letters, **47**:1019-1021.

Choi, Y. & Luong, H.C. 2001. A high-Q and wide-dynamic-range 70 MHz CMOS band-pass filter for wireless receivers. IEEE Transactions on Circuits and Systems II: Analog and Digital Signal Processing, **48**:433-440.

Córdova, D., Cruz, J. & Silva, C. 2009. A 2.3 GHz CMOS high-Q band-pass filter design using an active inductor. XV Workshop Iberchip Buenos Aires, Argentina, pp. 496-500.

Gao, Z., Ma, J., Yu, M. & Ye, Y. 2008. A fully integrated CMOS active band-pass filter for multiband RF front-ends IEEE Transactions on Circuits and Systems II: Express Briefs, **55**:718-722.

Idris, M.I.B., Reaz, M.B.I. & Bhuiyan, M.A.S. 2013. A low voltage VGA for RFID receivers, 2013 IEEE International Conference on RFID Technologies and Applications*,* Johor Bahru, Malaysia, pp. 1-4.

Krishnamurthy, S.V., El-Sankary, K. & El-Masry, E. 2010. Noise-cancelling CMOS active inductor and its application in RF band-pass filter design. International Journal of Microwave Science and Technology, **2010**:1-8.

Kuhn, W.B., Nobbe, D., Kelly, D. & Orsborn, A.W. 2003. Dynamic range performance of on-chip RF band-pass filters. IEEE Transactions on Circuits and Systems II: Analog and Digital Signal Processing, **50**:685-694.

Lin, L.M., Shun, W.H. & Tzuang, C.K.C. 2011. 1.58-GHz third-order CMOS active band-pass filter with improved passband flatness. IEEE Transactions on Microwave Theory and Techniques, **59**:2275-2284.

Ren, S. & Benedik, C. 2013. RF CMOS active inductor band pass filter with post fabrication calibration. AEU - International Journal of Electronics and Communications, **67**:1058-1067.

Rosli, K.A., Daud, R.M., Mamun, M. & Bhuiyan, M.A.S. 2013. A comparative study on SOI MOSFETs for low power applications. Research Journal of Applied Sciences, Engineering and Technology, **5**:2586-2591.

Uddin, M.J., Nordin, A.N., Reaz, M. & Bhuiyan, M.A.S. 2013. A CMOS power splitter for 2, 45 GHz ISM band RFID reader in 0, 18 µm CMOS technology. Tehnički vjesnik, **20**:125-129.

Wang, Y., Ye, L., Liao, H. & Huang, R. 2012. Cost-efficient CMOS RF tunable band-pass filter with active inductor-less biquads. 2012 IEEE International Symposium on Circuits and Systems (ISCAS), Seoul, pp. 2139-2142.

Weng, R. & Kuo, R. 2007. An ω 0-Q tunable CMOS active inductor for RF band-pass filters. 2007 International Symposium on Signals, Systems and Electronics (ISSSE'07), Montreal, pp. 571-574.

Wu, Y., Ding, X., Ismail, M. & Olsson, H. 2003. RF band-pass filter design based on CMOS active inductors. IEEE Transactions on Circuits and Systems II: Analog and Digital Signal Processing, **50**:942-949.

Xiao, H. & Schaumann, R. 2007. A 5.4-GHz high-Q tunable active-inductor band-pass filter in standard digital CMOS technology. Analog Integrated Circuits and Signal Processing, **51**:1-9.

Xu, Z., Winklea, D., Oh, T.C., Kim, S., Chen, S.T.W., Royter, Y., Lau, M., Valles, I., Hitko, D.A. & Li, J.C. 2014. A 5th order 0.8/2.4 GHz Programmable Active Band- pass Filter for Power DAC Applications. 2014 IEEE Radio Frequency Integrated Circuits Symposium, pp. 57-60.

Yu, C., Groves, R.A., Xuejue, H., Zamdmer, N.D., Plouchart, J.O., Wachnik, R.A., Tsu, K.J. & Chenming, H. 2003. Frequency-independent equivalent-circuit model for on-chip spiral inductors. IEEE Journal of Solid-State Circuits, **38**:419-426.

Submitted: 28/04/2015

Revised: 23/09/2015

Accepted: 05/04/2016